9 Scientific Essay: Thermalization and Localization

This essay will consider two states of the system: the Ergodic Phase (EP), also known as thermalized, and the Localized Phase (LP). We start with defining these two phases and their experimental observation in 1D and 2D, look at how interaction affects the formation of phases. Then after some numerical calculations[1] we will try to formulate the main markers of EP and LP, perhaps highlighting the factors influencing their formation. Finally, we will separately consider the issue of the influence of interaction on the growth of entanglement between subsystems. We will also compare Anderson Localization (AL) and Many Body Localization (MBL).

9.1 Intro

Model. We will study the effects of thermalization and localization using the Hubbard model

$$\hat{H} = -J \sum_{\langle i,j \rangle} (\hat{a}_i^\dagger \hat{a}_j + \text{h.c.}) + V \sum_{\langle i,j \rangle} \hat{n}_i \hat{n}_j + \Delta \sum_j \delta_j \hat{n}_j, \tag{1}$$

with V – nearest neighbor interaction, Δ – noise level, $\delta_j \in [-1, 1]$ evenly distributed (fig. 11c). To obtain numerical results, the hard-bosons limit is used (unless explicitly stated otherwise)[2]. This system is convenient in that we can look at various experimental implementations and all phases (EP and LP) of interest to us are implemented in it.

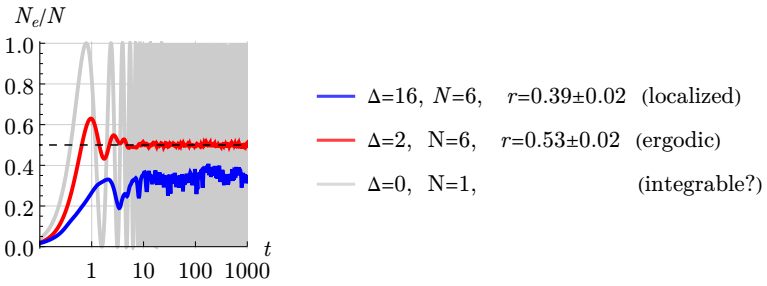

Figure 1: An example of different behavior scenarios for some observable .

Thermalization. Let's start by building some intuition about what could be called thermalization for an isolated quantum system [1]. Let the initial state be given by $|\psi_0\rangle$, then, in the basis of energy eigenstates $|j\rangle$, the evolution

$$|\psi(t)\rangle = \sum_{j=1}^{\mathcal{N}} c_j e^{-i\varepsilon_j t} |E_j\rangle$$

with $c_j = \langle E_j|\psi_0\rangle$, $\varepsilon_j = \langle j|\hat{H}|j\rangle$ and $\mathcal{N} = \dim H$. For some observable $\hat{A}(t)$ the mean value could be expressed as

$$A(t) = \langle\psi(t)|\hat{A}|\psi(t)\rangle = \sum_{j,k} \bar{c}_k c_j e^{-i(\varepsilon_j - \varepsilon_k)} \langle k|\hat{A}|j\rangle = \sum_j |c_j|^2 \langle j|\hat{A}|j\rangle + \sum_{k \neq j} c_j \bar{c}_k e^{-i(\varepsilon_j - \varepsilon_k)} \langle k|\hat{A}|j\rangle. \tag{2}$$

After some time of thermalization t_{th} we would like to see that the observables reach thermal values (independent of the initial conditions) with small fluctuations around (fig. 1, red curve)

$$A(t \gg t_{\text{th}}) = A(E) + \text{small fluctuations}, \qquad E = \langle\psi_0|\hat{H}|\psi_0\rangle.$$

To achieve small fluctuations around the average value, as we see from (2), it is enough to require the smallness of the off-diagonal elements[3]. And so that $A(E)$ does not depend on the initial conditions, we can consider the case when diagonal elements are smooth functions of energy

$$\langle j|\hat{A}|j\rangle = A(\varepsilon_j).$$

Indeed, then for the initial state lying in ΔE such that the spread $\partial_E A(E) \Delta E$ is small, the final result is

$$A(t \gg t_{\text{th}}) \approx \sum_j |c_j|^2 \langle j|\hat{A}|j\rangle \approx A(E).$$

This is how we come to the formulation of the Eigenstate Thermalization Hypothesis (ETH), put forward by Deutsch [2] and Srednicki [3]: if off-diagonal terms $\langle k|\hat{A}|j\rangle$ are small in compared to diagonal and diagonal terms are smooth

[1] Graphs from articles are accompanied by a link to the articles at the beginning, graphs without links are the results of my numerical modeling.

[2] The term $+\frac{1}{2}U \sum_j \hat{n}_j(\hat{n}_j - 1)$ was added to the Hamiltonian with $U \to \infty$.

[3] Note that the number of diagonal terms is $\mathcal{N}$ and off-diagonal $\mathcal{N}^2 - \mathcal{N}$. If we consider the contribution of each off-diagonal term to be random, then the fluctuations can be estimated as $\sqrt{\mathcal{N}^2}|\langle k|\hat{A}|j\rangle|$, which leads to to the requirement of smallness.

functions of energty, then the observed one seems to be thermalized. It is worth making some reservation that for an isolated system a pure state remains pure $\operatorname{tr}\rho^2 = 1$, while for a thermal state $\operatorname{tr}\rho^2 < 1$, which is why we talk about the thermalization of observables[4]. Again, judging by the conditions, it seems that systems and observables A_1, A_2 are possible such that A_1 is thermalized, but A_2 is not.

The main conclusion of this section: sometimes it happens that in some system and for some observable $\hat{A}$ its value $A(t \gg t_{\text{th}})$ reaches a constant with small fluctuations around, most likely this will correspond to the indicated ETH terms.

Localization. The fundamental opposite of thermalization is localization. It happens that the system retains information about the initial conditions even with $t \to \infty$ (fig. 1, blue curve) and $A = A(\psi_0)$. For example, we can divide the system into two equal subsystemsΩ_1, Ω_2, populate only Ω_1 and monitor the contrast

$$\mathcal{I} = \frac{N_{\Omega_1} - N_{\Omega_2}}{N_{\Omega_1} + N_{\Omega_2}}.$$

So in [4] in 1D the even lattice nodes (fig. 7) were chosen as Ω_1, and in [5] in 2D the left side of the system was taken as Ω_1 (fig.2). Just for $\mathcal{I}(t)$ the declared thermal behavior is already visible when $\mathcal{I}(t \gg t_{\text{th}}) \approx 0$, but at some point there is a transition to localization and $\mathcal{I}(t \gg t_{\text{th}}) \approx \text{const} > 0$. This behavior is typical when frozen noise $\Delta > 0$ is added to the system; this effect was first described by Anderson [6] for non-interacting particles (AL). In the case of interaction (MBL), the theoretical description, as far as I know, remains an open task and therefore is of great interest for experiment.

For a single-particle problem, it would be logical to assume that this behavior arises due to the localization of eigenfunctions. Indeed, in fig. 7 the eigenstates of the single-particle 1D Hamiltonian (1) are presented at different noise levels Δ.

9.2 MBL experiment in 2D

Let's consider the experimental implementation of the (1) system in [5] with approximately unity filled Mott insulator of bosonic ^{87}Rb atoms in a single plane of a cubic optical lattic.

To do this, by combining laser beams, we will obtain a certain interference pattern, the antinodes of which, at red detuning, will act as minima of the potential for atoms due to their polarizability (an alternative would be a lattice of optical tweeters). Between these potential minima, atoms will tunnel with a characteristic energy J (as in fig. 11c), which we will use as an energy scale. We can adjust the interaction U between atoms using Feischbach resonances, by turning it up to the value $U = 24J$ we get a system close to hard-bosons. We will apply a global harmonic potential on top of the grating, also by focusing the laser. Let's fill the trap with sufficiently cold atoms, using a microwave knife, leave only the left half filled and wait a little (fig. 2). Noises Δ are added to the system using DMD (alternatively, SLM, AOD or quasi-random potential are used as in [4], more details in [7]), the result is averaged over 50 implementations of δ_j.

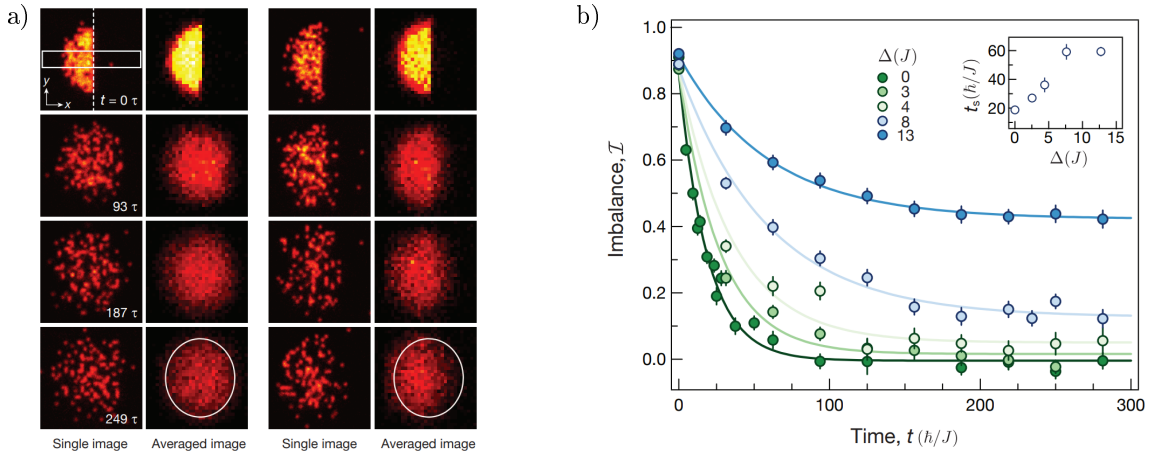

Figure 2: [5] a) Raw fluorescence images (red to yellow corresponds to increasing detected light level) showing the evolution of the initial density step without disorder. The left column shows the evolution with $\Delta = 0$ and the right column $\Delta = 13J$. b) Relaxation dynamics of a density domain wall.

[4] The hope arises that if we divide the system into two subsystems $\Omega_1 \cup \Omega_2$, then $\rho_1 = \operatorname{tr}_{\Omega_2}\rho$ can actually turn out to be thermal, and Ω_2 acts in some sense thermostat for Ω_1. This assumption will not be developed within the framework of this essay, but the I hope to return to this issue later.

It can be seen that in the absence of noise the system reaches a thermal state - thermalization ($\mathcal{I} \to 0$). With sufficiently strong noise, localization occurs: $\mathcal{I}(t \to \infty) = \mathcal{I}_\infty > 0$. Assuming the output to $\mathcal{I}_\infty$ to be exponential, we can notice how what is required to reach a steady state increases as the noise level increases.

It can also be seen that $\mathcal{I}_\infty > 0$ appears with $\Delta_c \approx 5.5(4)J$. The article emphasizes that Δ_c will increase as initial filling decreases. The clear difference in critical disorder strengths highlights the strong influence of interactions on the localization.

9.3 MBL experiment in 1D

To demonstrate the EP-LP transition, we can also consider an experiment on the implementation of a one-dimensional system [4] with degenerate Fermi gase of ^{40}K via sympathetic cooling with ^{87}Rb in a magnetic quadrupole and optical dipole trap followed by evaporative cooling.

Now we consider the motion in a quasi-random optical lattice created by two gratings with an incommensurate step, but in general still described by the Hamiltonian close to (1):

$$\hat{H} = -J \sum_{j,\sigma} \left(\hat{c}^\dagger_{j,\sigma} \hat{c}_{j+1,\sigma} + \text{h.c.} \right) + \Delta \sum_{j,\sigma} \cos(2\pi\beta j + \varphi) \hat{n}_{j,\sigma} + U \sum_j \hat{n}_{j,\uparrow} \hat{n}_{j,\downarrow},$$

with $\beta \in \mathbb{Q}$ to have quasi-random potential. A general view of the phase diagram is presented in fig. 11b.

Now odd nodes are chosen as Ω_1 and we also study how quickly and to what extent the contrast $\mathcal{I}$ of the population of even and odd nodes will disappear (fig. 3). It can be seen that for $t \approx 15\tau$ the observed $\mathcal{I}$ also reaches a stationary value (fig. 3a), where the dependence $\mathcal{I}(\Delta)$ (fig. 3b) is plotted based on the results of averaging in the yellow region.

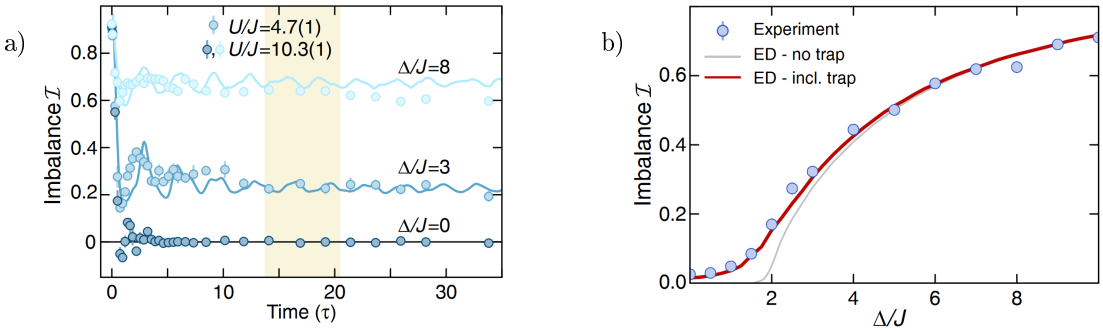

Figure 3: [4] a) Time evolution of an initial charge-density wave . b) Stationary values of the imbalance $\mathcal{I}$ as a function of disorder Δ for non-interacting atoms .

I the paper also measured the stationary value of $\mathcal{I}$ for different interactions U and different noise Δ (fig. 12b), in full accordance with the results of DMRG simulation [8]. It can be seen that LP is preserved in a wide range of interactions. The effect of interactions on the localization gives rise to a characteristic W-shape. It is also worth noting that the interaction leads to a logarithmic increase in the entropy of entanglement of subsystems (DMRG results at fig. 12a) , which we will return to in the corresponding section.

9.4 Numerical model in 2D

I was interested in looking at the behavior of a 2D system for the non-interacting case; a Gaussian packet lying entirely on the left side of the system was chosen as the initial state, and I also monitored the contrast $I(t)$. The presence of a global harmonic potential was described by a term of the form $\sum_j u_j \hat{n}_j$. Evolution was considered through ED (Exact Diagonalization) and expansion of the initial state into its own (fig. 4a). Similarly, at a small noise level the system was thermalized, and at large values it reached a localized state.

In the thermalizing state, the result is statistically significant and does not depend on the initial state (results not presented here). It is interesting to look at the resulting distribution of node population $\langle n_j \rangle_t$, averaged over time, from the energy of this node $\delta_j + u_j$ (fig. 4c). It is also interesting to compare $\langle n_j \rangle_t$ with the resulting thermal distribution $\operatorname{tr} n_j e^{-\beta H}$, I obtained the correlation coefficient

$$\operatorname{corr}\left(\langle n_j \rangle_t, \operatorname{tr} n_j e^{-\beta H}\right)|_{\Delta=0.5} \approx 0.8, \qquad \operatorname{corr}\left(\langle n_j \rangle_t, \operatorname{tr} n_j e^{-\beta H}\right)|_{\Delta=5} \approx 0.2,$$

which is quite consistent with the ideas of localization and thermalization.

A natural question arises: how exactly can one characterize the localization phase and the ergodic phase (thermalizing) of a system, and what algorithm can be fed with the Hamiltonian. Various metrics are presented in [9], but the best place to start is the r-parameter, which is the focus of the next section.

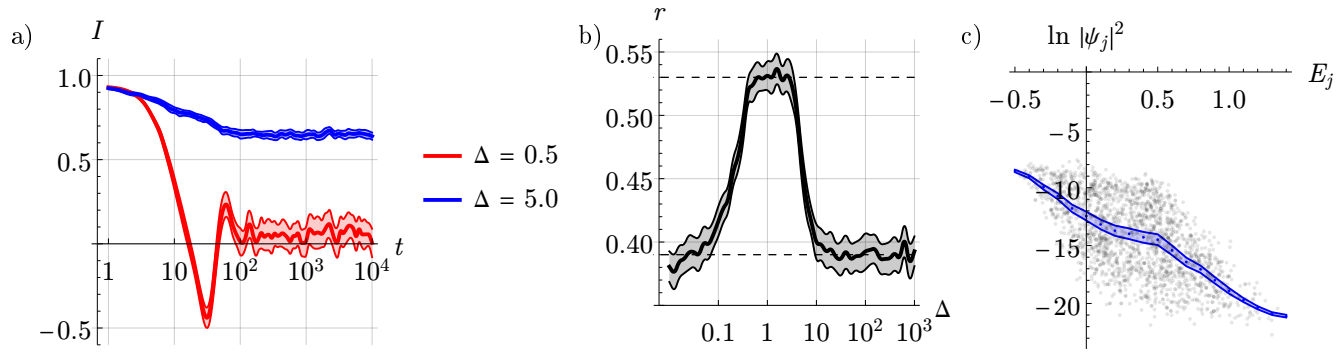

Figure 4: a) Evolution of contrast $I(t)$ averaged over 50 realizations δ_j for two noise levels Δ: thermalization and localization. b) Dependence of r-parameter on the noise level Δ, averaged over 50 realizations of δ_j. c) For a thermalized state, the dependence of the population of the node $|\psi_j|^2$ on the energy of the node $E_j = \delta_j + u_j$, black dots indicate the dependence for a specific implementation δ_j, blue indicates the result of averaging over 50 implementations.

9.5 Random Matrices

Let's consider the following procedure: for some matrix M, find all eigenvalues λ_j, ordered in ascending order, and determine the r-parameter [10]

$$r \stackrel{\text{def}}{=} \left\langle \frac{\min(\delta_j, \delta_j + 1)}{\max(\delta_j, \delta_{j+1})} \right\rangle_j, \qquad \delta_j = \lambda_{j+1} - \lambda_j. \tag{3}$$

We can immediately note several such properties that it is not sensitive to transformations of the form $M \to \alpha_1 M + \alpha_2 \mathbb{1}$, moreover, as we will notice later, it is not sensitive to many things.

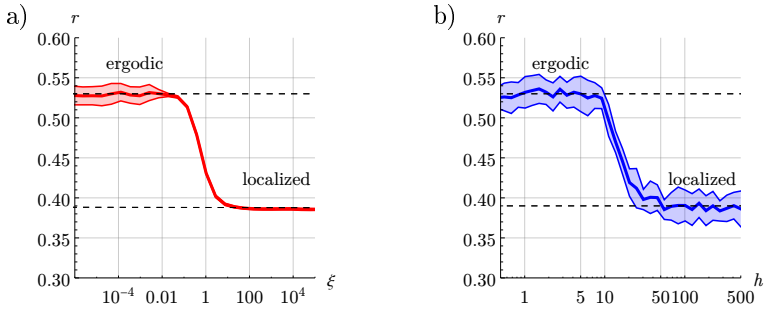

Figure 5: a) Phase transition EP-LP with random matrix. b) Phase transition EP-LP with 1D hard-bosons (1), $h \equiv \Delta$

Now let's take a closer look at the (1) system and the phase transition that occurs when Δ increases. In coordinate representation, noise is simply a random diagonal addition to the Hamiltonian[5]. Thus, for $\Delta \gg J$ (at least in the single-particle case), the Hamiltonian is practically diagonalized (fig. 7). On the other side there is a non-diagonal part, for which J is responsible. The paper [10] proposes to model this phase transition using two random matrices: a random Hermitian M_1 (GOE) and a random diagonal M_2, thus $M = (1-k)M_1 + kM_2$. The limiting values $k = 0$ and $k = 1$ characterize chaotic and nonchaotic regimes (thermalizing and localizing). To ensure that the transition does not depend on the parameters $M_{1,2}$, we can scale k as

$$\xi = \frac{1}{D} \frac{k\sigma_2}{(1-k)\sigma_1},$$

where $\sigma_{1,2}$ are the standard deviation of elements in $M_{1,2}$ respectively and D is the size of the matrix.

We can find $r(\xi)$ for matrices with $D = 200$, $\sigma_1 = \sigma_2 = 1$ (for other values the dependence is the same), averaging the result over 100 implementations (fig. 5a). For comparison, the dependence of $r(\xi)$ is given for a 1D system (1) hard-bosons for noise level h (the same as Δ) on the lattice with $L = 14$ half-fill sites[6] (7 particles). According to [10, 9] the value $r \approx 0.53$ is a marker of the ergodic phase (a characteristic value for GOE), and $r \approx 0.39$ is a marker

[5] You need to be careful here, because as we will see later, small changes in the diagonal through $V \neq 0$ lead to fundamentally different behavior of the system [11].

[6] If we were talking about the Heisenberg model, then this would correspond to a complete spin equal to zero.

of the localized phase (the so-called Poisson statistics):

$$\boxed{r \approx 0.53 - \text{ergodic}} \qquad \boxed{r \approx 0.39 - \text{localized}}$$

I note that it is the word marker that is used, since these conditions are neither necessary nor sufficient.

A similar dependence will be obtained if we consider as M_1 the connectivity matrix of a random graph (a Hermitian matrix with random elements $0, 1$). Considering that on average there are θ non-zero elements per line, we can ask the question about the influence of θ on the formation of the ergodic phase (fig. 6a). If θ is too small, the probability of Hilbert Space Fragmentation [12] is high, which obviously cannot lead to thermalization of the system. Moreover, the system does not thermalize when it is integrated [13].

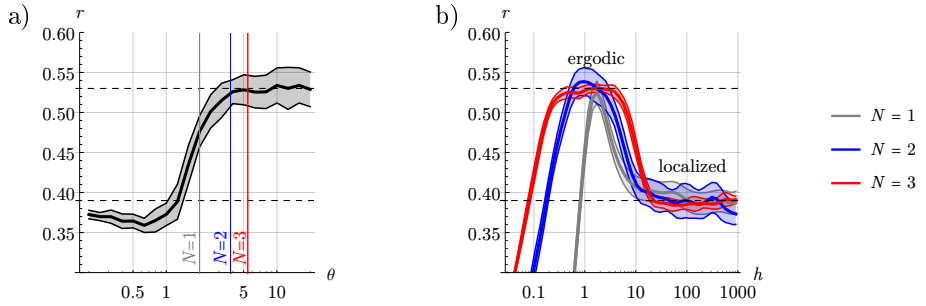

Figure 6: a) The influence of matrix rarefaction θ on phase formation with $\xi = 0.01$. b) Phase transition with 1D hard-bosons with $L = 20$.

I paid such attention to θ and fragmentation, since this in some sense helps to understand why for a small number of particles in the system the ergodic phase (judging by r) practically does not occur (fig. 6). Indeed, with a smaller number of particles ($N = 1, 2, 3$) and the same lattice size $L = 14$, the Hamiltonian is more rarefied (fig. 6a), Hilbert Space Fragmentation occurs (that is the Hamiltonian can be represented in block diagonal form) and, accordingly, thermalization does not occur.

The main conclusion of this section: the r-parameter is quite universal in nature and can be used as a marker of the ergodic phase and localized phase. The EP-LP phase transition can be modeled by random matrices (GOE, random diagonal, random graph adjacency matrix).

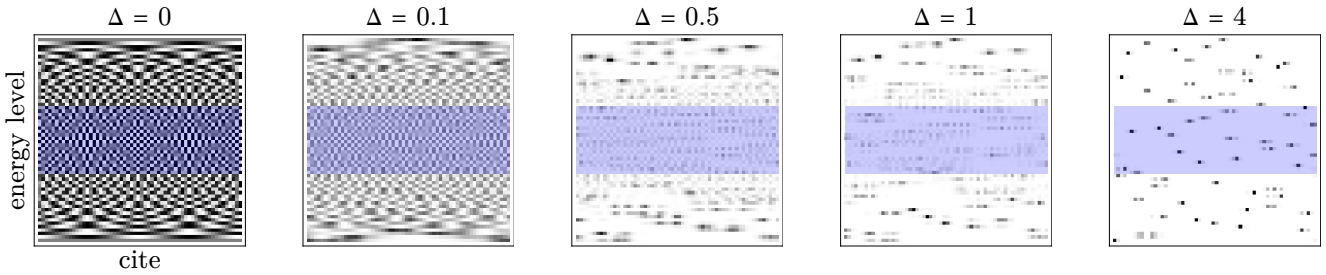

Figure 7: The eigenstates $|\psi_j\rangle$ of the single-particle 1D Hamiltonian (1) onto gratings of length $L = 60$, the color indicates the value $|\psi_j|^2$. It can be seen that localization occurs immediately for the ground state, but in the area highlighted in blue, localization occurs later.

9.6 Numerical model in 1D

As can be seen from fig. 7 localization depends on temperature: for the system under consideration, low-energy states are localized first, and then the middle of the spectrum (the area highlighted in blue in fig. 7). The article [9] specifically examines the occurrence of localization at $\beta = 0$, that is, when in a thermal state all states are equally probable (however, for purity, all metrics will be calculated in the middle third of the spectrum). The system is considered to be a Heisenberg chain with random fields along the z-direction

$$\hat{H} = J \sum_{j=1}^{L} \hat{\boldsymbol{S}}_j \cdot \hat{\boldsymbol{S}}_{j+1} + \sum_{j=1}^{L} h_j \hat{S}_j^z,$$

for zero total spin, which is generally almost equivalent to the Hubbard hard-boson model and $h_j \in [-h, h]$. A phase transition is detected in the system at (or crossover?) at $h = h_c = (3.5 \pm 1)\,J$. The system is quite exotic in that we see a quantum phase transition at a non-zero temperature, and even in one dimension. To a large extent, this is possible precisely due to the lack of ergodicity in the system.

The article performs Exact Diagonalization (ED) for $J = 8, 10, \ldots, 16$. A phase transition is detected (fig. 8a) by the already familiar r-parameter (3). Also, for all results, averaging is carried out over noise realizations.

It is also proposed to consider the decay of the longest wavelength disturbance of the spin density

$$\hat{M} = \sum_j \hat{S}^z_j \exp\left(i\frac{2\pi j}{L}\right).$$

Consider an initial condition that is at infinite temperature, but with a small modulation of the spin density in this mode, so the initial density matrix is $\rho_0 = (\mathbb{1} + \epsilon\hat{M}^\dagger)/Z$. For such an initial condition $\langle\hat{M}\rangle_0 = \mathrm{tr}(\rho_0\hat{M})$. The long-time average of the spin polarization in this mode is

$$\langle\hat{M}\rangle_t = \frac{\epsilon}{Z}\sum_n \langle n|\hat{M}^\dagger|n\rangle\langle n|\hat{M}^\dagger|n\rangle.$$

They define the fraction of the contribution to the initial polarization that is dynamic and thus decays away (on average) at long time, as

$$f^{(n)} = 1 - \frac{\langle n|\hat{M}^\dagger|n\rangle\langle n|\hat{M}^\dagger|n\rangle}{\langle n|\hat{M}^\dagger\hat{M}|n\rangle}.$$

In the ergodic phase, the system does thermalize, so the initial polarization does relax away and $f \to 1$. In the localized phase, on the other hand, there is no long-distance spin transport, so $f \to 0$. Это и наблюдается (fig. 8a).

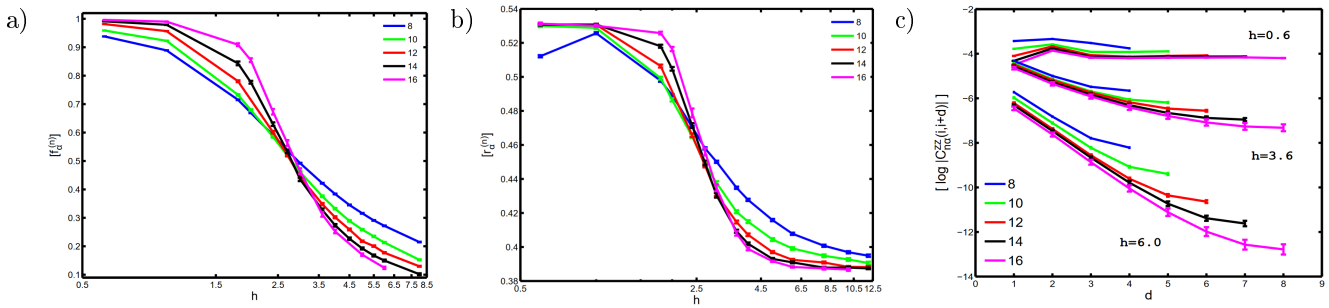

Figure 8: [9] a) The fraction of the initial spin polarization that is dynamic. b) The ratio of adjacent energy gaps (r-parameter). c) The spin-spin correlations in the manybody eigenstates as a function of the distance d.

Another way to detect a phase transition is to see that for large noises the correlations begin to decay exponentially

$$C_n(i,j) = \langle n|\hat{S}^i_z\hat{S}^j_z|n\rangle - \langle n|\hat{S}^i_z|n\rangle\langle n|\hat{S}^z_j|n\rangle,$$

where the average value $\langle\log|C_n(i, i+d)|\rangle_{i,n,h_j}$ is displayed (fig. 8c).

9.7 Entropy growth

The last topic I want to focus on in this essay is the effect of entropy on the growth of entanglement between subsystems. Let us select a subsystem Ω_1 in the system $\Omega = \Omega_1 \cup \Omega_2$. The entropy of the subsystem can be found through the reduced density matrix $\rho_{\Omega_1} = \mathrm{tr}_{\Omega_2}\,\rho$

$$S(\rho_{\Omega_1}) = -\,\mathrm{tr}\,\rho_{\Omega_1}\ln\rho_{\Omega_1},$$

one shows that bipartite entanglement exists between two disjoint subsystems Ω_1 and Ω_2 of Ω with reduced density matrices ρ_{Ω_1} and ρ_{Ω_2} if

$$S(\rho_{\Omega_1}) > S(\rho_{\Omega_1\cup\Omega_2}) \qquad \text{or} \qquad S(\rho_{\Omega_2}) > S(\rho_{\Omega_1\cup\Omega_2}).$$

However, further we will simply monitor the growth of the entropy of the subsystem, which in general most likely indicates the entanglement of the subsystems. We will also work with one-dimensional chain hard-bosons described by the Hamiltonian (1). Let us divide the system into two parts: left and right; as the initial state we will consider half population at even nodes (fig. 9). The growth of entropy in LP is considered. It can be seen that the addition of a weak interaction leads to a statistically significant increase in entropy. In my opinion, this is a rather non-obvious result, since the interaction is a small diagonal addition to the Hamiltonian, which already has random numbers on the diagonals.

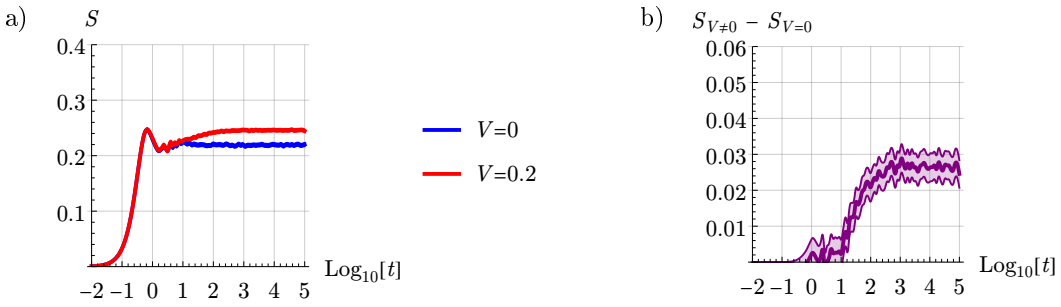

Figure 9: a) Entanglement growth. b) The same data but with subtracted values.

Similar results were obtained in [11]. As in [4] (fig. 12a), a logarithmic increase in entropy is observed (fig. 10a). Since the calculations in the article were carried out through ED, rather small systems were considered, which led to the constant S (fig. 10b), however, an obvious trend can be traced as the size of the system increases.

Thus, at least from the point of view of entanglement and entropy of subsystems, MBL is fundamentally different from AL. The entanglement increases slowly until a saturation time scale, which diverges in the infinite system.

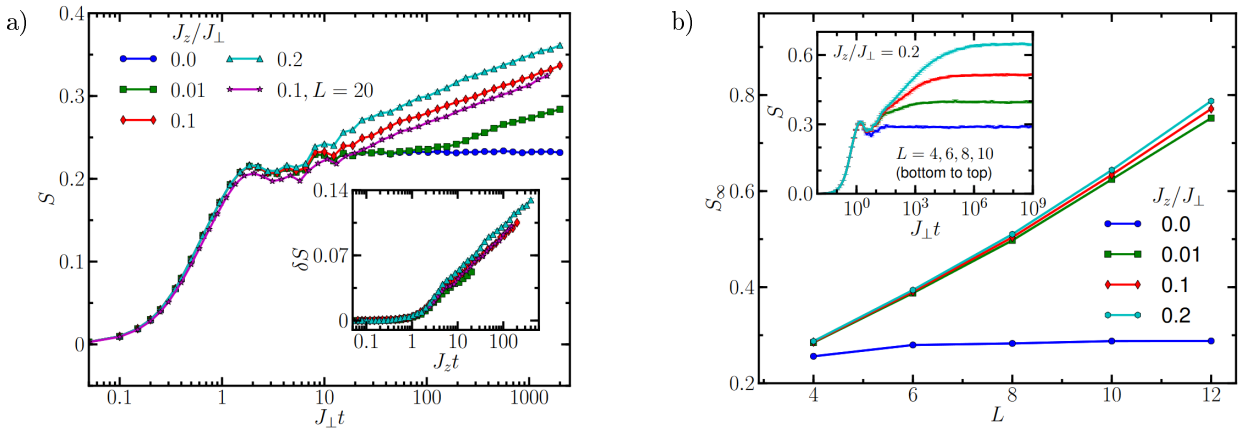

Figure 10: [11] a) Entanglement growth. b) Saturation values of the entanglement entropy as a function of L.

9.8 Conclusion

Experimental implementations and numerical simulations of EP and LP in the Hubbard model (or in 1D Heisenberg model) in 1D and 2D for the non-interacting case (EP-LP:AL) and the interacting case (EP-LP:MBL) are considered. For a many-particle problem, the Hamiltonian is less sparse; Hilbert Space Fragmentation, but thermalization usually occurs. A shift in the critical noise level required for transition to LP was observed due to the presence of interactions between particles. Also, fundamentally different behavior was observed in MBL compared to AL in terms of the growth of entanglement and entropy of subsystems.

9.9 Supplementary Material

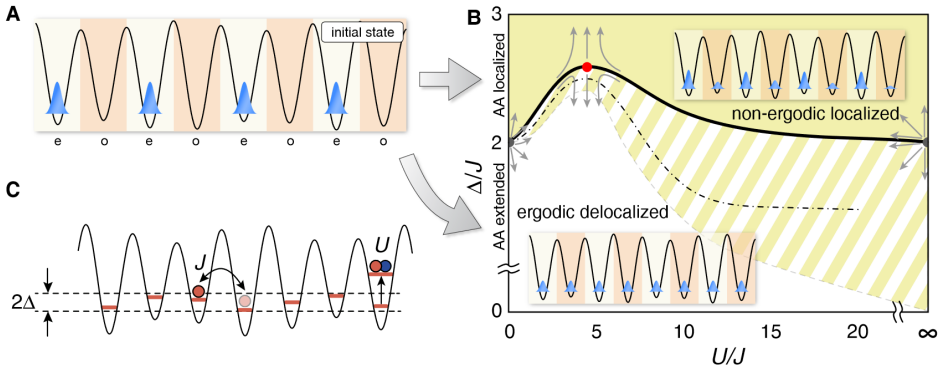

Figure 11: [4] 1D system (1). a) Initial state of the system consisting of a charge density wave, where all atoms occupy even sites only. For an interacting many-body system, the evolution of this state over time depends on whether the system is ergodic or not. b) Schematic phase diagram for the system: in the ergodic, delocalized phase (white) the initial state quickly decays, while it persists for long times in the non-ergodic, localized phase (yellow). c) Schematic showing a visual representation of the three terms in the Hamiltonian (1).

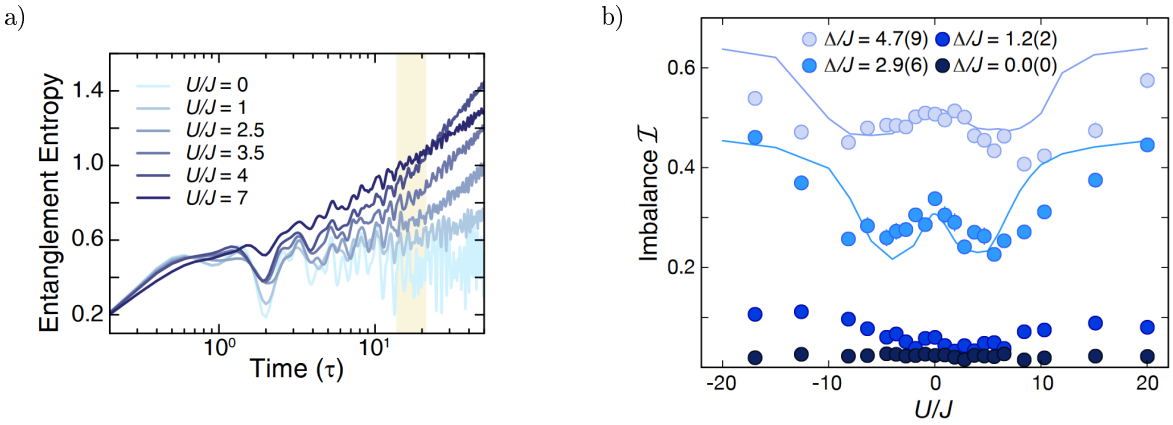

Figure 12: [4] a) DMRG results of the entanglement entropy growth for various interaction strengths and $\Delta = 5J$. For long times, logarithmic growth characteristic of interacting MBL states is visible. b) Cuts along four different disorder strengths. The effect of interactions on the localization gives rise to a characteristic W-shape. Solid lines are the results of DMRG simulations for a single homogeneous tube.

References

[1] Sergei Khlebnikov and Martin Kruczenski. Thermalization of isolated quantum systems, March 2014.

[2] J. M. Deutsch. Quantum statistical mechanics in a closed system. *Phys. Rev. A*, 43:2046–2049, Feb 1991.

[3] Mark Srednicki. Chaos and quantum thermalization. *Phys. Rev. E*, 50:888–901, Aug 1994.

[4] Michael Schreiber, Sean S. Hodgman, Pranjal Bordia, Henrik P. Lüschen, Mark H. Fischer, Ronen Vosk, Ehud Altman, Ulrich Schneider, and Immanuel Bloch. Observation of many-body localization of interacting fermions in a quasi-random optical lattice. *Science*, 349(6250):842–845, August 2015.

[5] Jae-yoon Choi, Sebastian Hild, Johannes Zeiher, Peter Schauß, Antonio Rubio-Abadal, Tarik Yefsah, Vedika Khemani, David A. Huse, Immanuel Bloch, and Christian Gross. Exploring the many-body localization transition in two dimensions. *Science*, 352(6293):1547–1552, June 2016.

[6] P. W. Anderson. Absence of diffusion in certain random lattices. *Phys. Rev.*, 109:1492–1505, Mar 1958.

[7] Dmitry A. Abanin, Ehud Altman, Immanuel Bloch, and Maksym Serbyn. Many-body localization, thermalization, and entanglement. *Reviews of Modern Physics*, 91(2):021001, May 2019.

[8] Steven R. White. Density matrix formulation for quantum renormalization groups. *Phys. Rev. Lett.*, 69:2863–2866, Nov 1992.

[9] Arijeet Pal and David A. Huse. The many-body localization phase transition. *Physical Review B*, 82(17):174411, November 2010.

[10] Xingbo Wei, Rubem Mondaini, and Gao Xianlong. Characterization of many-body mobility edges with random matrices, January 2020.

[11] Jens H. Bardarson, Frank Pollmann, and Joel E. Moore. Unbounded growth of entanglement in models of many-body localization. *Physical Review Letters*, 109(1):017202, July 2012.

[12] Sanjay Moudgalya, B Andrei Bernevig, and Nicolas Regnault. Quantum many-body scars and hilbert space fragmentation: a review of exact results. *Reports on Progress in Physics*, 85(8):086501, July 2022.

[13] Marcos Rigol, Vanja Dunjko, and Maxim Olshanii. Thermalization and its mechanism for generic isolated quantum systems. *Nature*, 452(7189):854–858, April 2008.